

Repurposing the diuretic benzamil as an anti-osteosarcoma agent that acts by suppressing integrin/FAK/STAT3 signalling and compromising mitochondrial function

Cite this article:
Bone Joint Res 2024;13(4):
157–168.

DOI: 10.1302/2046-3758.
134.BJR-2023-0289.R1

Correspondence should be
sent to Bor-Chyuan Su
subc8265@tmu.edu.tw

M-C. Lin,¹ G-Y. Chen,¹ H-H. Yu,^{2,3} P-L. Hsu,^{4,5} C-W. Lee,⁶ C-C. Cheng,² S-Y. Wu,⁷ B-S. Pan,⁸ B-C. Su^{9,10}

¹School of Medical Laboratory Science and Biotechnology, College of Medical Science and Technology, Taipei Medical University, Taipei, Taiwan

²Division of General Surgery, Department of Surgery, Wan Fang Hospital, Taipei Medical University, Taipei, Taiwan

³Division of General Surgery, Department of Surgery, School of Medicine, College of Medicine, Taipei Medical University, Taipei, Taiwan

⁴Department of Anatomy, School of Medicine, College of Medicine, Kaohsiung Medical University, Kaohsiung, Taiwan

⁵Department of Medical Research, Kaohsiung Medical University Hospital, Kaohsiung, Taiwan

⁶Department of Nursing, National Tainan Junior College of Nursing, Tainan, Taiwan

⁷Department of Cancer Biology, Wake Forest Baptist Medical Center, Wake Forest University, Winston-Salem, North Carolina, USA

⁸Department of Pathology, Duke University School of Medicine, Durham, North Carolina, USA

⁹Department of Anatomy and Cell Biology, School of Medicine, College of Medicine, Taipei Medical University, Taipei, Taiwan

¹⁰Graduate Institute of Medical Sciences, College of Medicine, Taipei Medical University, Taipei, Taiwan

Aims

Osteosarcoma is the most common primary bone malignancy among children and adolescents. We investigated whether benzamil, an amiloride analogue and sodium-calcium exchange blocker, may exhibit therapeutic potential for osteosarcoma *in vitro*.

Methods

MG63 and U2OS cells were treated with benzamil for 24 hours. Cell viability was evaluated with the MTS/PMS assay, colony formation assay, and flow cytometry (forward/side scatter). Chromosome condensation, the terminal deoxynucleotidyl transferase dUTP nick end labelling (TUNEL) assay, cleavage of poly-ADP ribose polymerase (PARP) and caspase-7, and FITC annexin V/PI double staining were monitored as indicators of apoptosis. Intracellular calcium was detected by flow cytometry with Fluo-4 AM. The phosphorylation and activation of focal adhesion kinase (FAK) and signal transducer and activator of transcription 3 (STAT3) were measured by western blot. The expression levels of X-linked inhibitor of apoptosis protein (XIAP), B-cell lymphoma 2 (Bcl-2), B-cell lymphoma-extra large (Bcl-xL), SOD1, and SOD2 were also assessed by western blot. Mitochondrial status was assessed with tetramethylrhodamine, ethyl ester (TMRE), and intracellular adenosine triphosphate (ATP) was measured with BioTracker ATP-Red Live Cell Dye. Total cellular integrin levels were evaluated by western blot, and the expression of cell surface integrins was assessed using fluorescent-labelled antibodies and flow cytometry.

Results

Benzamil suppressed growth of osteosarcoma cells by inducing apoptosis. Benzamil reduced the expression of cell surface integrins $\alpha 5$, αV , and $\beta 1$ in MG63 cells, while it only reduced the expression of αV in U2OS cells. Benzamil suppressed the phosphorylation and activation of FAK and STAT3. In addition, mitochondrial function and ATP production were compromised by benzamil. The levels of anti-apoptotic proteins XIAP, Bcl-2, and Bcl-xL were reduced by benzamil. Correspondingly, benzamil potentiated cisplatin- and methotrexate-induced apoptosis in osteosarcoma cells.

Conclusion

Benzamil exerts anti-osteosarcoma activity by inducing apoptosis. In terms of mechanism, benzamil appears to inhibit integrin/FAK/STAT3 signalling, which triggers mitochondrial dysfunction and ATP depletion.

Article focus

- To investigate the cytotoxic activity of benzamil on human osteosarcoma cells.
- To investigate the molecular mechanism by which benzamil mediates the anticancer activity of human osteosarcoma cells.

Key messages

- Benzamil-induced cytotoxicity is not limited to osteosarcoma cells with certain phenotypes.
- Benzamil inhibits integrin/focal adhesion kinase (FAK)/signal transducer and activator of transcription 3 (STAT3) signalling and induces mitochondrial damage.
- Benzamil potentiates cisplatin- and methotrexate-induced apoptosis.

Strength and limitations

- Our results uncover a potential new application of benzamil as an osteosarcoma treatment.
- Only in vitro experiments were performed; further in vivo studies are warranted to confirm the applicability in clinical settings.

Introduction

Osteosarcoma is the most common malignant bone tumour in children and young adults.¹ While the condition can occur in any bone, it is mostly long tubular bones that are affected.² Currently, the primary therapeutic approaches for osteosarcoma include amputation, chemotherapy, and radiotherapy.¹ Amputation is mostly used in child patients rather than in adults; it provides a substantial survival benefit, yet it causes functional impairment of the affected limb and has no benefit with regard to incidence of local recurrence.³⁻⁵ To restore the adequate function, limb salvage surgery is also performed. When amputation is performed in combination with adjuvant chemotherapy, the five-year survival rate is greatly improved in non-metastatic osteosarcoma patients.¹ However, the survival benefit is not extended to patients with metastatic disease.⁴ The most common and effective chemotherapy regimen for osteosarcoma is a combination of methotrexate, adriamycin, and cisplatin,⁶ which is associated with major adverse effects including hearing loss, bone marrow suppression, renal toxicity, liver damage, and cardiomyopathy.⁷ To resolve these adverse effects, discontinuation of treatment

is often required.⁸ Furthermore, the efficacy of the chemotherapy regimen varies greatly due to the high genetic and phenotypic heterogeneity among osteosarcoma cases.^{9,10} To make matters worse, nearly 35% of osteosarcoma patients experience local or systemic recurrence despite having received amputation and chemotherapy.¹¹ Radiotherapy is not commonly used to treat osteosarcoma, since the tumours are largely radio-insensitive.¹ As such, radiotherapy is only used to treat patients who have a poor response to chemotherapy or for whom surgery cannot be performed adequately.^{1,5,12} In light of the difficulties in treating osteosarcoma, there is an urgent need to identify new agents that can overcome the major challenges in osteosarcoma treatment.

In this study, we evaluate the potential of benzamil, a derivative of amiloride, as a treatment for osteosarcoma. Benzamil is a potent sodium-calcium exchanger blocker that also exhibits diuretic activity.¹³ Its inhibitory activity on sodium-calcium exchange is ten times more potent than that of amiloride.¹⁴ Like amiloride, benzamil is sometimes used to treat cystic fibrosis lung disease, although its therapeutic efficacy is not better than amiloride.¹⁵ In addition to these known activities, recent work has shown that benzamil may have anticancer activity in the context of human brain cancer.¹⁶ The main reported mechanism of its cytotoxicity to cancer cells was disturbance of intracellular calcium balance.¹⁶ We hypothesized that benzamil might induce cytotoxicity via elevation of intracellular calcium and calcium-related mechanisms in osteosarcoma cells. In the present study, we explored the anticancer effects of benzamil in osteosarcoma cells and delineated the underlying mechanisms of its cytotoxic effects.

Methods

Reagents

Benzamil was purchased from Cayman Chemical (USA), and 4',6'-diamidino-2-phenylindole (DAPI), propidium iodide (PI), 2',7'-dichlorodihydrofluorescein diacetate (DCFDA), crystal violet, glutaraldehyde, BAPTA, Y15, BioTracker ATP-Red Live Cell Dye, and cisplatin were purchased from Millipore-Sigma (USA). Tetramethylrhodamine, ethyl ester (TMRE) was purchased from Thermo Fisher Scientific (USA). Stattic was purchased from MedChemExpress (USA). FITC annexin V was purchased from BioLegend (USA). MTS and PMS were purchased from Promega (USA). Fluo-4 AM was purchased from Abcam (USA).

Cell culture and treatment

The human osteosarcoma cell lines, MG63 and U2OS, were purchased from the Bioresource Collection and Research Centre (Taiwan). Cells were maintained in Dulbecco's Modified Eagle Medium (DMEM) supplemented with 10% fetal bovine serum (Peak, USA), penicillin, and streptomycin (Sartorius, Germany). The cell cultures were incubated at 37°C in a culture incubator with 5% CO₂. To validate the dose-dependent effect of benzamil on anti-osteosarcoma activities, cells were treated with 0, 12.5, 25, 50, 100, and 200 μM benzamil for 24 hours. To assess the time course of benzamil-induced apoptosis and the underlying mechanisms, cells were treated with 200 μM benzamil for 0, 0.5, one, three, six, and 24 hours. To validate the requirement of calcium in benzamil-induced apoptosis, cells were preincubated with BAPTA (20 μM) for one hour, followed by benzamil (100 μM) for 24 hours. Apoptosis was validated by FITC annexin V/PI double staining. To address the roles of focal adhesion kinase (FAK) and signal transducer and activator of transcription 3 (STAT3) in benzamil-induced apoptosis, cells were treated with Y15 (10 μM) and Stattic (20 μM) for 24 hours. Apoptosis was validated by FITC annexin V/PI double staining. To investigate the enhancement of apoptotic effects of cisplatin by benzamil, cells were preincubated with cisplatin (10 μM) or methotrexate (30 μM) for one hour, followed by benzamil (75 μM) for 24 hours. Apoptosis was validated by FITC annexin V/PI double staining. Vehicle control: 0.5% dimethyl sulfoxide (DMSO).

Cell viability assay

MG63 cells were seeded onto a 96-well plate at a density of 8,000 cells/well. Cells were treated with 0, 12.5, 25, 50, 100, and 200 μM benzamil for 24 hours. Cell viability was assessed with the MTS/PMS assay, according to the manufacturer's instructions (Promega). Absorbance at 490 nm was measured using a SpectraMax ABS microplate reader (Molecular Devices, USA).

Colony formation assay

The colony formation assay was performed as described previously.¹⁷ Briefly, MG63 and U2OS cells were seeded into six-well plates (300 cells/well) and incubated at 37°C for five hours. After the cells were firmly attached to the dish, the cultures were treated with indicated doses of benzamil for 24 hours. At the end of the treatment period, the medium was removed and fresh medium was added. Culture medium was subsequently refreshed every three days. On day 9, colonies were fixed with 6% glutaraldehyde and stained with 0.5% crystal violet for observation. Images of the colonies were obtained using scanning devices (MPC3503; Ricoh, Japan).

Forward and side scatter analysis

Forward scatter (FSC) and side scatter (SSC) were analyzed using flow cytometry (Beckman Coulter, USA). FSC/SSC indexes were used to identify living and/or dead cells according to standard protocols.¹⁸

Apoptosis analysis

Apoptosis was analyzed by chromatin condensation, terminal deoxynucleotidyl transferase dUTP nick end labelling (TUNEL) assay, cleavage of poly-ADP ribose polymerase (PARP) and caspase-7, and FITC annexin V/PI double staining. Chromatin condensation was assessed as previously described.¹⁹ Briefly,

the MG63 cells were seeded into a 48-well plate at a density of 30,000 cells/well. Cells were treated with 100 μM benzamil for 24 hours. Then, cells were fixed by 4% formaldehyde for 30 minutes. After the fixative was removed, the cells were stained with DAPI for 20 minutes. Chromatin condensation was observed and scored using fluorescence microscopy (Motic, China). The TUNEL assay was performed according to the manufacturer's instructions (Abcam). Cleavage of PARP and caspase-7 was monitored by western blot analysis. FITC annexin V/PI double staining was performed as previously described.¹⁹ After the cells were stained, the samples were analyzed by flow cytometry (Beckman Coulter).

Western blot analysis

MG63 (4 × 10⁵ cells/ml) and U2OS (6 × 10⁵ cells/ml) were seeded into six-well plates. Cells were treated with indicated doses of benzamil for 24 hours. Cells were lysed and collected in RIPA buffer (MilliporeSigma) supplemented with cComplete Protease Inhibitor Cocktail (Roche, Switzerland) and PhosSTOP (Roche). Thereafter, cell lysates were separated on a gradient gel, and proteins were transferred onto a 0.22 μm polyvinylidene difluoride (PVDF) membrane (Cytiva, USA). Protein expression was detected by using the indicated primary antibody and appropriate secondary antibody. Bands were visualized using ECL horseradish peroxidase (HRP) substrate (MilliporeSigma). Band intensity was measured from images using ImageJ bundled with 64-bit Java 8 (National Institutes of Health, USA). Briefly, each band's intensity was quantified. Then, the target band intensities were divided by the β-actin intensities. All primary antibodies used in this study were purchased from Cell Signaling Technology (USA), including anti-caspase-7 (9492), anti-PARP (9542), anti-phospho-FAK (3283), anti-FAK (3285), anti-phospho-STAT3 (9145), anti-STAT3 (9139), anti-X-linked inhibitor of apoptosis protein (XIAP) (2042), anti-B-cell lymphoma 2 (Bcl-2) (4223), anti-B-cell lymphoma-extra large (Bcl-XL) (2764), anti-SOD1 (2770), anti-SOD2 (13194), anti-integrin α5 (4705), anti-integrin αV (4711), anti-integrin β1 (9699), and anti-β-actin (3700). The secondary antibody used for anti-STAT3 and anti-β-actin was peroxidase-AffiniPure goat anti-mouse immunoglobulin G (IgG) (115-035-003; Jackson ImmunoResearch, USA). Except for these two, the secondary antibody used for other primary antibodies was peroxidase-AffiniPure goat anti-rabbit IgG (111-035-003; Jackson ImmunoResearch).

Mitochondrial membrane potential, ROS, ATP, and calcium analysis

Mitochondrial membrane potential was assessed according to the TMRE signal measured by flow cytometry (Beckman Coulter), as previously described.²⁰ The reactive oxygen species (ROS) level was detected by measuring DCFDA signal with flow cytometry (Beckman Coulter). Briefly, cells were loaded with DCFDA (10 μM) for 20 minutes. Then, cells were rinsed with phosphate-buffered saline (PBS) three times. The fluorescence intensity of DCFDA was measured by flow cytometry. To measure intracellular adenosine triphosphate (ATP), BioTracker ATP-Red Live Cell Dye was used. Cells were incubated with BioTracker ATP-Red Live Cell Dye (10 μM) for 15 minutes. Then, the cells were rinsed with PBS three times. The fluorescence intensity of BioTracker ATP-Red Live Cell Dye was measured by flow cytometry. In order to

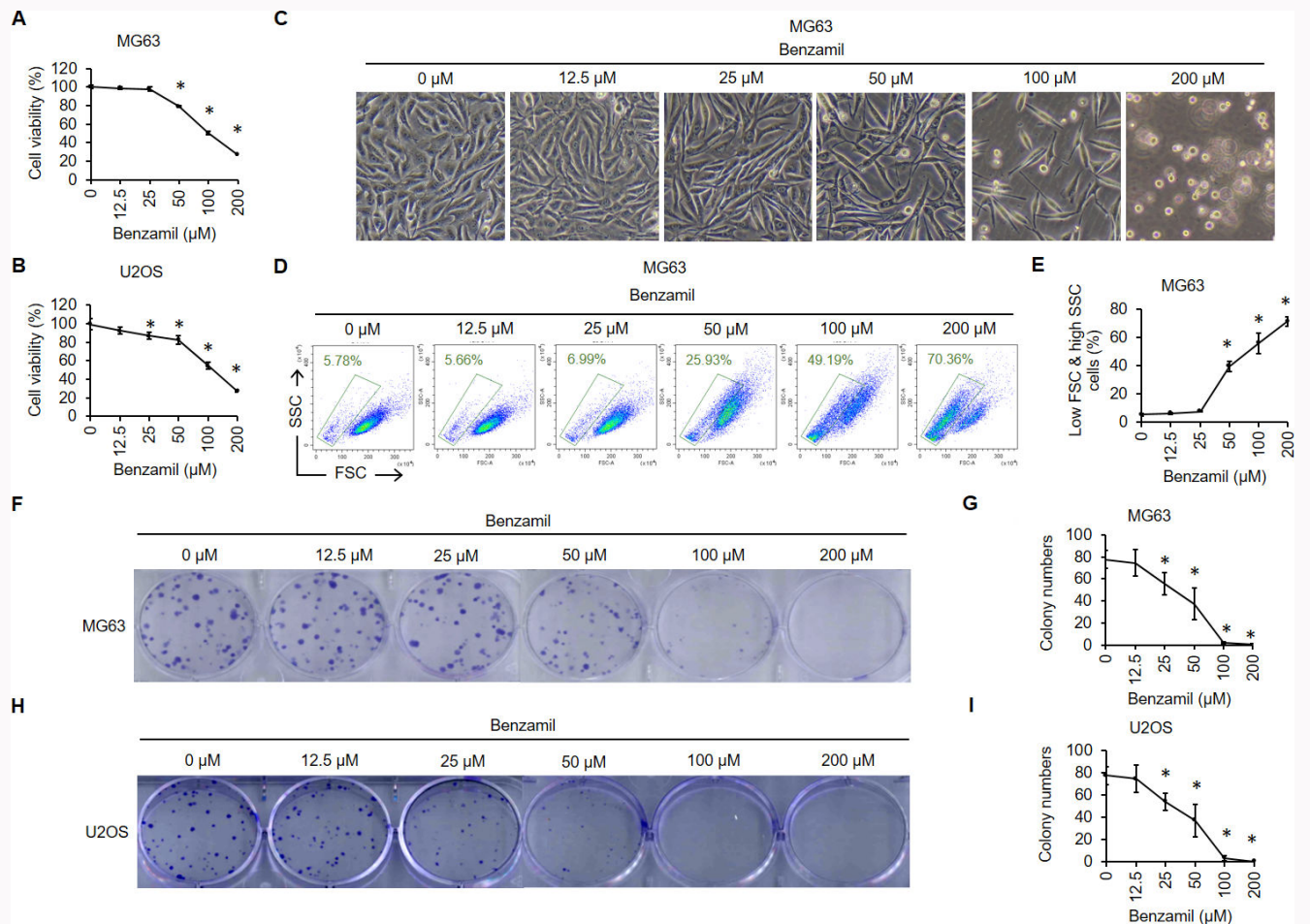


Fig. 1 Benzamil dose-dependently reduces cell viability in vitro. MTS/PMS activity assay of a) MG63 and b) U2OS cells after treatment with the indicated doses of benzamil for 24 hours. c) MG63 cells were treated with indicated doses of benzamil for 24 hours. Cell morphology was observed under light microscopy. d) MG63 cells were treated as described in c); forward scatter (FSC) and side scatter (SSC) were analyzed by flow cytometry. e) Percentage of gated cells (low FSC and high SSC). f) to i) Colony formation assay with MG63 (f and g) and U2OS (h and i) cells after treatment with the indicated doses of benzamil. * $p < 0.05$ comparing indicated dose with 0 μM , one-way analysis of variance.

examine the intracellular calcium levels, cells were preloaded with the fluorescent calcium indicator Fluo-4 AM (2 μM) for 15 minutes, followed by benzamil treatment. Excess Fluo-4 AM dye was washed away with PBS washing, and the fluorescence intensity of Fluo-4 AM was measured by flow cytometry.

Surface integrin analysis

After treatment, cells were collected using trypsin (Sartorius) and washed with PBS (Sartorius). Then, the cells were stained with the indicated integrin antibody (integrin $\alpha 5$ -FITC, integrin αV -FITC, and integrin $\beta 1$ -Alexa Fluor 488) at 4°C for one hour. After the cells were rinsed with PBS three times, the fluorescence intensity was measured by flow cytometry.

Statistical analysis

All experiments were performed in triplicate with at least three independent replicates. Experimental results are expressed as mean and standard error of the mean (SEM). Statistical significance was validated by independent-samples t -test or one-way analysis of variance (ANOVA). Significant differences are indicated as $p < 0.05$. All statistics were calculated using GraphPad Prism 8 (GraphPad Software, USA).

Results

Benzamil reduces cell viability of osteosarcoma cells

In order to test whether benzamil has a cytotoxic effect in human osteosarcoma cells, MG63 (Figure 1a) and U2OS (Figure 1b) cells were treated with different doses of benzamil for 24 hours. Cell viability was then measured by the MTS/PMS assay. Cytotoxicity was detected when MG63 cells were exposed to at least 50 μM benzamil (0 μM vs 50 μM : mean 100 (SEM 1.6) vs 79 (SEM 1), $p < 0.001$) and when U2OS cells were exposed to 25 μM benzamil (0 μM vs 50 μM : mean 100 (SEM 5.3) vs 86 (SEM 3.5), $p < 0.05$, one-way ANOVA). Morphological examinations also revealed that the numbers of rounded cells (apoptotic feature) were increased when MG63 cells were exposed to benzamil (Figure 1c). We also analyzed the change in cell morphology using flow cytometry. The percentage of cells with morphological features of a dead cell (low FSC and high SSC)^{18,21} was greatly increased by benzamil treatment (0 μM vs 50 μM : mean 5.2% (SEM 0.7%) vs 40% (SEM 3.7%), $p < 0.001$; 0 μM vs 100 μM : mean 5.2% (SEM 0.7%) vs 56% (SEM 7.3%), $p < 0.001$; 0 μM vs 200 μM : mean 5.2% (SEM 0.7%) vs 71% (SEM 3.2%), $p < 0.001$, one-way ANOVA) (Figures 1d and 1e). The colony formation assay confirmed that growth of MG63 (Figures 1f and 1g) and U2OS

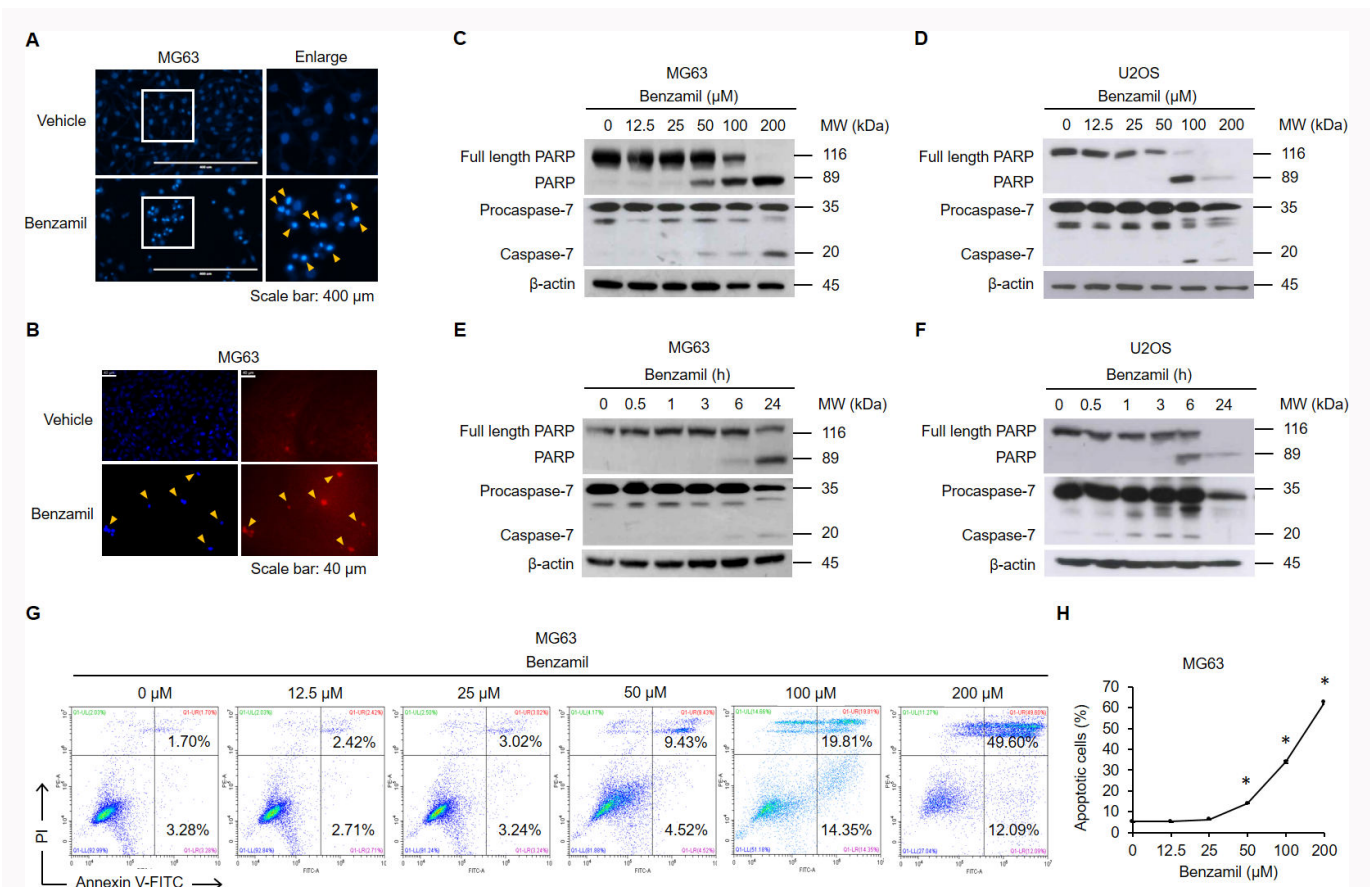


Fig. 2

Benzamil dose-dependently induces apoptosis. MG63 cells were treated with benzamil (100 μM) for 24 hours. Apoptosis was detected according to: a) chromosome condensation assay; and b) terminal deoxynucleotidyl transferase dUTP nick end labelling (TUNEL) assay. c) MG63 and d) U2OS cells were treated with indicated doses of benzamil for 24 hours. Poly-ADP ribose polymerase (PARP) cleavage and caspase-7 activation were examined by western blot analysis. e) MG63 and f) U2OS cells were treated with benzamil (200 μM) for 0, 0.5, one, three, six, and 24 hours. PARP cleavage and caspase-7 activation were examined by western blot analysis. g) MG63 cells were treated with indicated doses of benzamil for 24 hours. Apoptosis was analyzed by FITC annexin V/PI double staining. h) Quantification of apoptosis. Cells represented in the lower right (early apoptosis) and upper right (late apoptosis) quadrants of the graph were defined as apoptotic cells. * $p < 0.05$ comparing indicated dose with 0 μM, one-way analysis of variance.

(Figures 1h and 1i) cells was inhibited when the cultures were exposed to at least 25 μM benzamil (MG63: 0 μM vs 25 μM: mean 77 (SEM 8) vs 55 (SEM 10), $p = 0.040$; U2OS: 0 μM vs 25 μM: mean 78 (SEM 8) vs 54 (SEM 7), $p = 0.020$, one-way ANOVA).

Benzamil induces apoptosis in osteosarcoma cells

To examine whether apoptosis is induced by benzamil, cells were treated with benzamil for 24 hours. Apoptosis was evaluated by chromosome condensation (Figure 2a)^{19,22} and the TUNEL assay (Figure 2b). The results showed that benzamil treatment increased the numbers of cells with condensed chromosomes and TUNEL-positive signals. Next, MG63 (Figure 2c) and U2OS (Figure 2d) cells were treated with different doses of benzamil, and apoptosis was examined by cleavage of PARP and caspase-7.²³ We found that both PARP and caspase-7 were cleaved after benzamil treatment. Subsequently, MG63 (Figure 2e) and U2OS (Figure 2f) cells were treated with benzamil for 0, 0.5, one, three, six, and 24 hours. Cleavage of PARP and caspase-7 was examined by western blot, which revealed that benzamil induces cleavage of PARP and caspase-7 within only a few hours. Interestingly, we found that the levels of cleaved PARP and caspase-7

were lower in U2OS cells treated with 200 μM benzamil for 24 hours compared with the 100 μM dose or six hours (Figures 2d and 2f). This result might be due to the fact that apoptotic proteases are quickly degraded after their activation.²⁴ Moreover, MG63 cells were treated with increasing doses of benzamil for 24 hours, and apoptosis was measured by FITC annexin V and PI double staining (Figures 2g and 2h). As expected, we found that benzamil induces apoptosis of MG63 cells in a dose-dependent manner (0 μM vs 50 μM: mean 5.2 (SEM 0.3) vs 14 (SEM 0.13), $p < 0.001$; 0 μM vs 100 μM: mean 5.2 (SEM 0.3) vs 34 (SEM 0.4), $p < 0.001$; 0 μM vs 200 μM: mean 5.2 (SEM 0.3) vs 62.5 (SEM 0.9), $p < 0.001$, one-way ANOVA).

Calcium is not essential for benzamil-induced cytotoxicity

Since benzamil cytotoxicity in human brain tumour cells is mediated by elevation of intracellular calcium,¹⁶ we next tested whether calcium is also involved in benzamil-induced apoptosis of osteosarcoma cells. Similar to the findings of a previous study,¹⁶ our data showed that benzamil elevates the intracellular calcium level in MG63 cells (vehicle vs benzamil: mean 1 (SEM 0.01) vs 1.4 (SEM 0.09), $p = 0.002$, independent-samples t-test) (Figure 3a). However, addition of the calcium chelator BAPTA had minimal or no effect on benzamil-induced

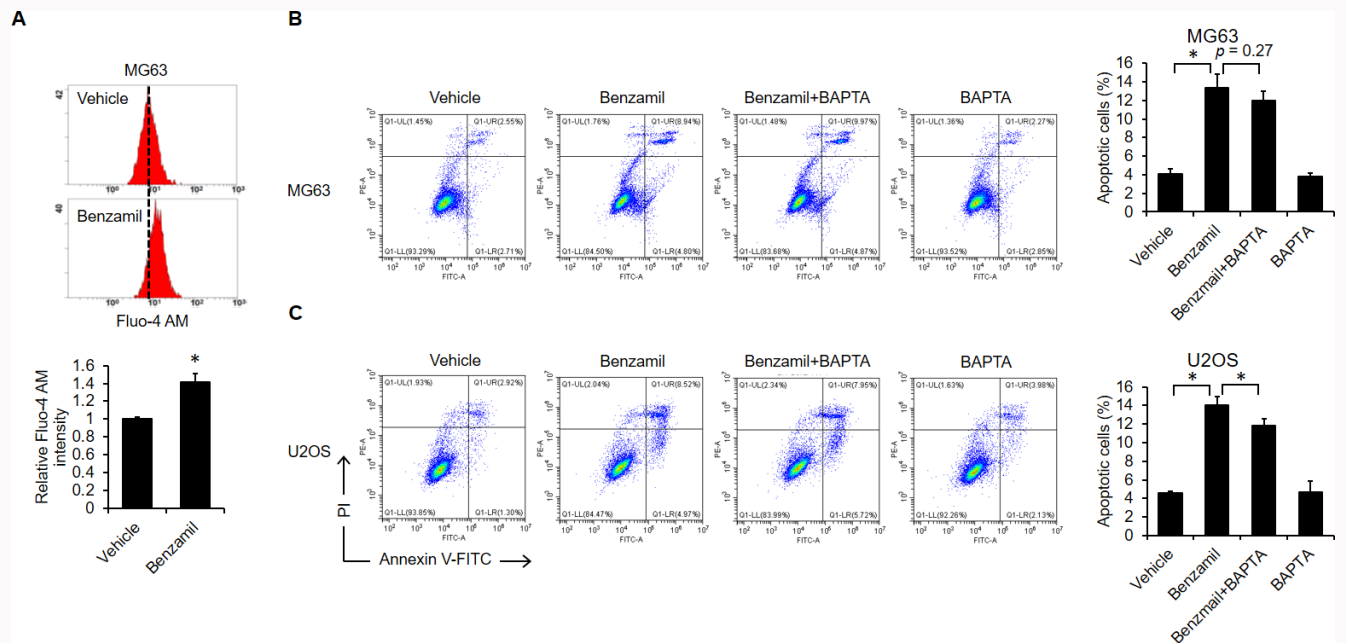


Fig. 3

Calcium elevation is not required for benzamil cytotoxicity. a) MG63 cells were treated with benzamil (100 μ M) for six hours. Intracellular calcium level was analyzed using Fluo-4 AM by flow cytometry. Mean fluorescence intensity of Fluo-4 AM was quantified. b) MG63 and c) U2OS cells were preincubated with BAPTA (20 μ M) for one hour, followed by benzamil (100 μ M) for 24 hours. Apoptosis was analyzed by FITC annexin V/PI double staining. * $p < 0.05$ (A: independent-samples t -test; B&C: one-way analysis of variance). Vehicle: 0.5% dimethyl sulfoxide.

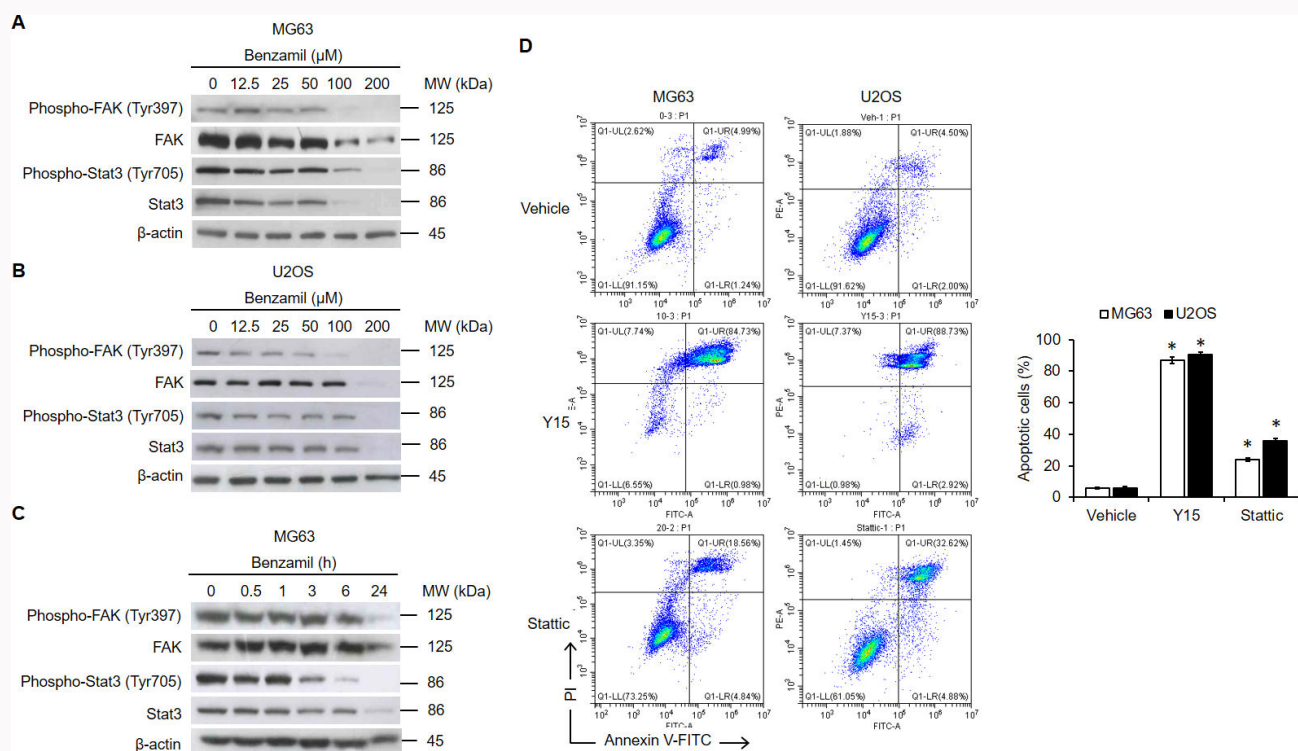


Fig. 4

Benzamil reduces phosphorylation and activation of focal adhesion kinase (FAK) and signal transducer and activator of transcription 3 (STAT3). a) MG63 and b) U2OS cells were treated with indicated doses of benzamil for 24 hours. Phosphorylation and activation of FAK and STAT3 were measured by western blot analysis. c) MG63 cells were treated with benzamil (200 μ M) for 0, 0.5, one, three, six, and 24 hours. Phosphorylation and activation of FAK and STAT3 were measured by western blot analysis. d) MG63 and U2OS cells were treated with Y15 (10 μ M) and Stattic (20 μ M) for 24 hours. Apoptosis was analyzed by FITC annexin V/PI double staining. * $p < 0.05$ comparing the indicated group with the vehicle group, independent-samples t -test. Vehicle: 0.5% dimethyl sulfoxide.

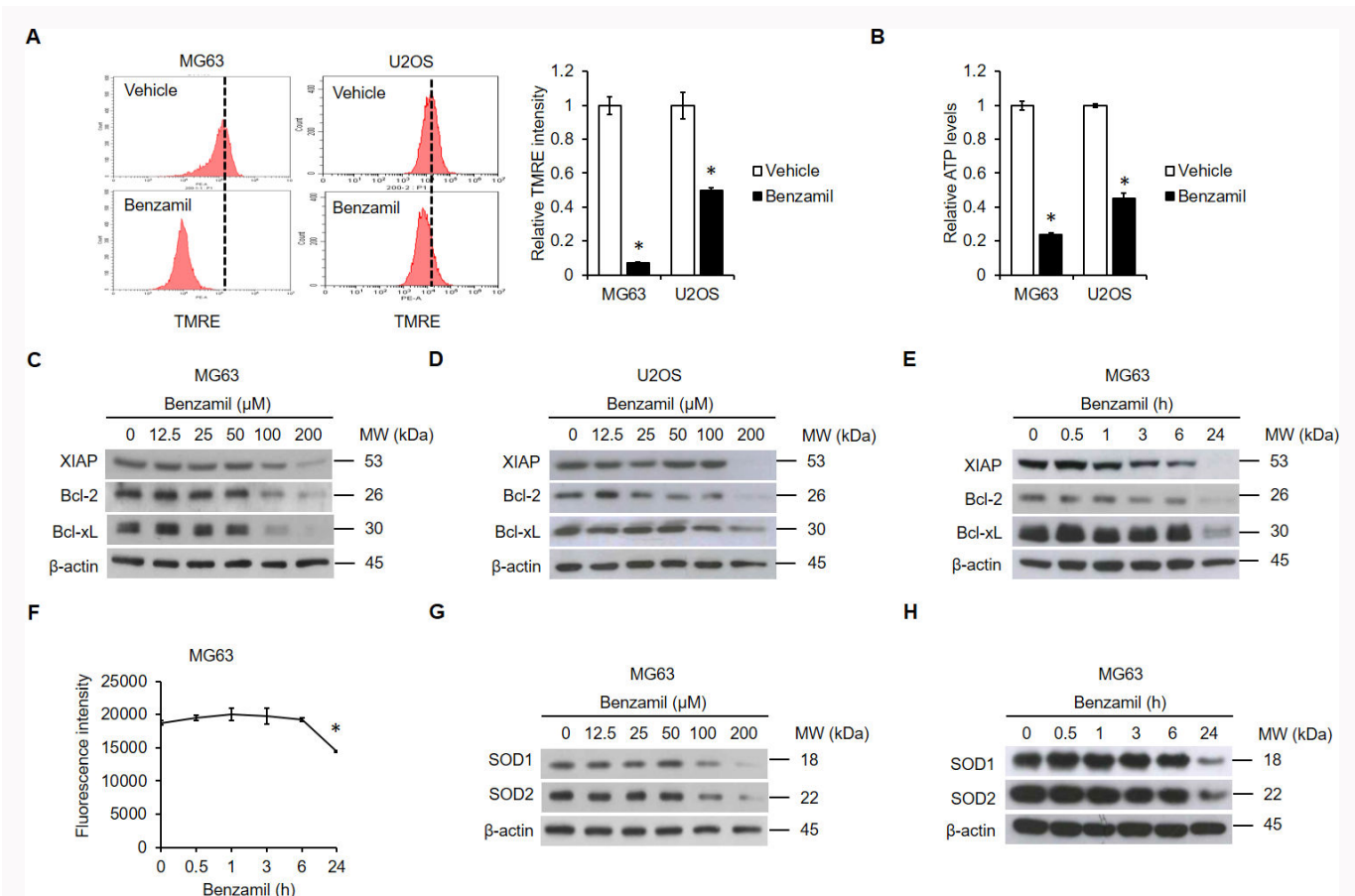


Fig. 5

Benzamil causes decreases in mitochondria membrane potential, anti-apoptotic proteins, and intracellular reactive oxygen species (ROS). a) MG63 and U2OS cells were treated with benzamil (200 μ M) for 24 hours. Mitochondria membrane potential was analyzed by tetramethylrhodamine, ethyl ester (TMRE) staining. TMRE fluorescence intensity was measured by flow cytometry. b) MG63 and U2OS cells were treated with benzamil (200 μ M) for 24 hours. Intracellular adenosine triphosphate (ATP) was detected with BioTracker ATP-Red Live Cell Dye (10 μ M) using flow cytometry. c) MG63 and d) U2OS cells were treated with indicated doses of benzamil for 24 hours. The levels of X-linked inhibitor of apoptosis protein (XIAP), B-cell lymphoma 2 (Bcl-2), and B-cell lymphoma-extra large (Bcl-xL) were examined by western blot. e) MG63 cells were treated with benzamil (200 μ M) for 0, 0.5, one, three, six, and 24 hours. The levels of XIAP, Bcl-2, and Bcl-xL were examined by western blot. f) MG63 cells were treated with benzamil (200 μ M) for 0, 0.5, one, three, six, and 24 hours. Intracellular ROS was analyzed by 2',7'-dichlorodihydrofluorescein diacetate (DCFDA). Fluorescence intensity of DCFDA was measured by flow cytometry. g) MG63 cells were treated with indicated doses of benzamil for 24 hours. The levels of SOD1 and SOD2 were examined by western blot. h) MG63 cells were treated with benzamil (200 μ M) for 0, 0.5, one, three, six, and 24 hours. The levels of SOD1 and SOD2 were examined by western blot. * $p < 0.05$ comparing indicated group to vehicle group (A and B: independent-samples t -test; F: one-way analysis of variance). Vehicle: 0.5% dimethyl sulfoxide.

apoptosis in MG63 (benzamil vs benzamil+BAPTA: mean 13.3 (SEM 1.5) vs 12 (SEM 1), $p = 0.270$, independent-samples t -test) (Figure 3b) and U2OS (benzamil vs benzamil+BAPTA: mean 14 (SEM 1) vs 11.8 (SEM 0.76), $p = 0.040$, independent-samples t -test) (Figure 3c) cells. Thus, our findings suggest that calcium is unlikely to play an essential role in benzamil-induced apoptosis in osteosarcoma cells.

Benzamil suppresses FAK/STAT3 pathways

FAK and STAT3 are often overexpressed in osteosarcoma and implicated in cancer progression.^{25,26} However, the effects of benzamil on these two signalling molecules remain unclear. Therefore, we examined the dose and time course effects of benzamil on these two signalling molecules in osteosarcoma cells. Our results showed that both phosphorylation and activation of FAK and STAT3 were suppressed by benzamil in MG63 (Figure 4a) and U2OS (Figure 4b) cells. In particular, activation and phosphorylation of FAK were suppressed in MG63 cells exposed to benzamil for 24 hours (Figure 4c), while

activation and phosphorylation of STAT3 were inhibited after exposing MG63 cells to benzamil for three hours. To further examine the importance of FAK and STAT3 in osteosarcoma cell survival, MG63 and U2OS cells were treated with Y15 (FAK inhibitor) and Stattic (STAT3 inhibitor); then, apoptosis was measured by flow cytometry (Figure 4d). The results showed that inhibition of FAK and STAT3 could indeed lead to apoptosis (MG63: vehicle vs Y15: mean 5.7 (SEM 0.6) vs 87 (SEM 2), $p < 0.001$; vehicle vs stattic: mean 5.7 (SEM 0.6) vs 24 (SEM 1), $p < 0.001$; U2OS: vehicle vs Y15: mean 6 (SEM 1) vs 91 (SEM 1.5), $p < 0.001$; vehicle vs stattic: mean 6 (SEM 1) vs 36 (SEM 1.5), $p < 0.001$, independent-samples t -test). Taken together, these results imply that benzamil might induce apoptosis at least partially via suppression of FAK and STAT3.

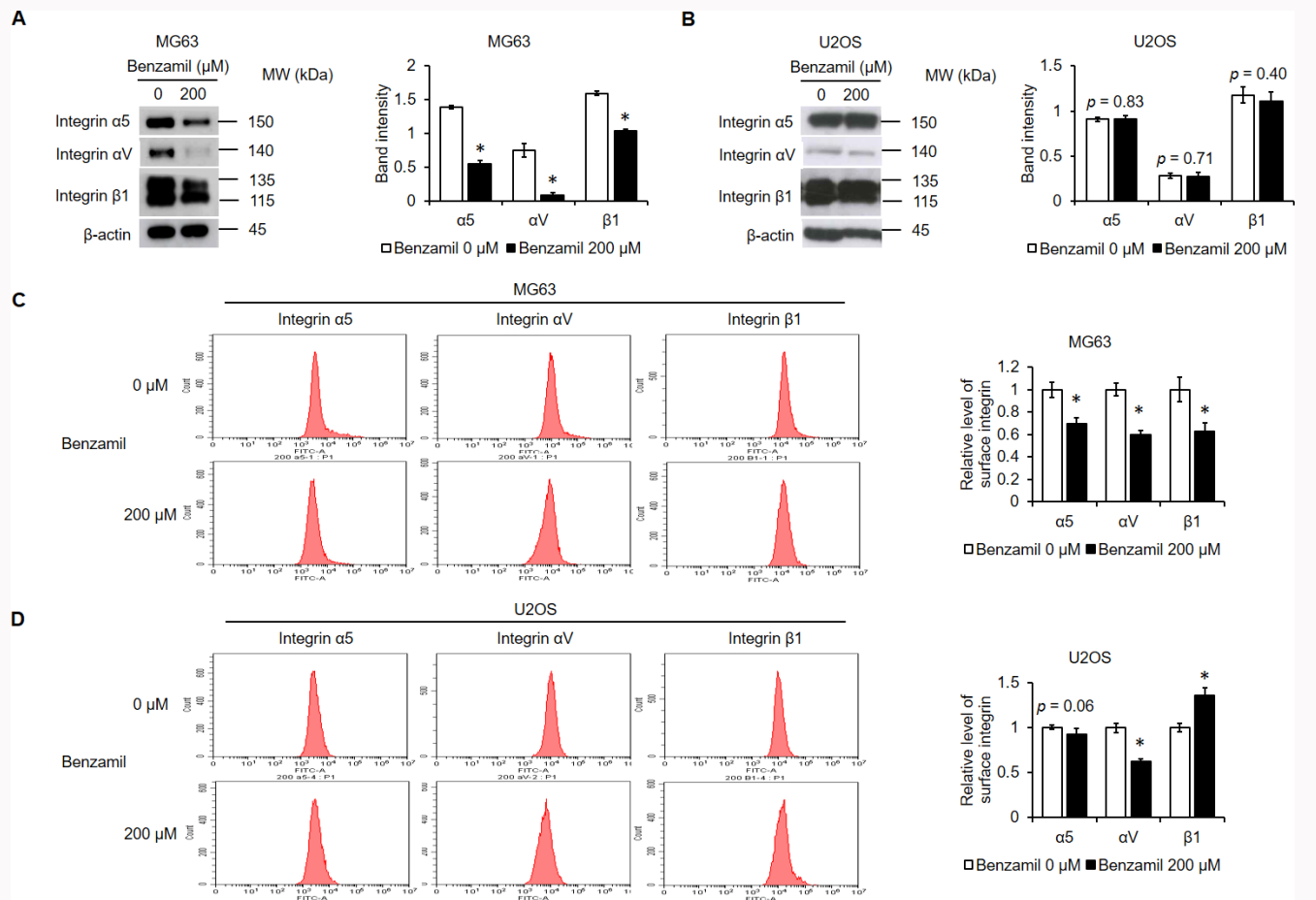


Fig. 6 Benzamil alters integrin expression profile. a) MG63 and b) U2OS cells were treated with benzamil (200 μM) for 24 hours. The levels of integrin α5, integrin αV, and integrin β1 were examined by western blot. c) MG63 and d) U2OS cells were treated with benzamil (200 μM) for 24 hours. The cell surface levels of integrin α5, integrin αV, and integrin β1 were examined by flow cytometry. **p* < 0.05 (independent-samples *t*-test): statistically significant compared to vehicle.

Benzamil triggers mitochondrial dysfunction and suppresses anti-apoptotic and anti-oxidant proteins

Since FAK/STAT3 signalling promotes cell survival via its regulation of mitochondrial function,²⁷ we next wanted to test the effect of benzamil on mitochondrial status in MG63 and U2OS cells (Figure 5a). Intriguingly, benzamil treatment greatly reduced the intensity of TMRE in both MG63 and U2OS cells (MG63: vehicle vs benzamil: mean 1 (SEM 0.05) vs 0.07 (SEM 0.005), *p* < 0.001; U2OS: vehicle vs benzamil: mean 1 (SEM 0.07) vs 0.5 (SEM 0.02), *p* < 0.001, independent-samples *t*-test), suggesting that the drug induces mitochondrial hypopolarization. We also found that the intracellular ATP level was dramatically reduced by benzamil (MG63: vehicle vs benzamil: mean 1 (SEM 0.03) vs 0.24 (SEM 0.008), *p* < 0.001; U2OS: vehicle vs benzamil: mean 1 (SEM 0.009) vs 0.45 (SEM 0.03), *p* < 0.001, independent-samples *t*-test) (Figure 5b). Taken together, these data are consistent with the idea that mitochondrial ATP production is inhibited by benzamil. Next, the effects of benzamil on anti-apoptotic proteins (XIAP, Bcl-2, and Bcl-xL) were examined. We found that benzamil reduces the levels of XIAP, Bcl-2, and Bcl-xL in both MG63 (Figure 5c) and U2OS (Figure 5d) cells. Furthermore, the data showed that these anti-apoptotic proteins were all strongly suppressed after 24 hours of exposure to benzamil (Figure 5e).

We also found that the levels of intracellular ROS (0 hrs vs 24 hrs: mean 18,723 (SEM 327) vs 14,398 (SEM 136), *p* < 0.001, one-way ANOVA) (Figure 5f) and antioxidative proteins (SOD1 and SOD2) (Figures 5g and 5h) were suppressed by benzamil.

Benzamil changes integrin expression profile

To explore the effect of benzamil on the expression profile of integrins at a total cellular protein level, MG63 (Figure 6a) and U2OS (Figure 6b) cells were treated with benzamil, and the levels of integrin α5, αV, and β1 were measured by western blot. Benzamil treatment reduced the levels of all integrins in MG63 cells (integrin α5: 0 μM vs 200 μM: mean 1.39 (SEM 0.02) vs 0.55 (SEM 0.04), *p* < 0.001; integrin αV: 0 μM vs 200 μM: mean 0.75 (SEM 0.1) vs 0.08 (SEM 0.04), *p* < 0.001; integrin β1: 0 μM vs 200 μM: mean 1.59 (SEM 0.03) vs 1.03 (SEM 0.02), *p* < 0.001, independent-samples *t*-test). However, this suppressive effect was not observed in U2OS cells. We next tested the effect of benzamil specifically on the cell surface integrin expression profile by flow cytometry. Our results showed that benzamil also suppressed the cell surface expression of all integrins in MG63 cells (integrin α5: 0 μM vs 200 μM: mean 1 (SEM 0.07) vs 0.7 (SEM 0.05), *p* = 0.003; integrin αV: 0 μM vs 200 μM: mean 1 (SEM 0.05) vs 0.59 (SEM 0.03), *p* < 0.001; integrin β1: 0 μM vs 200 μM: mean 1 (SEM

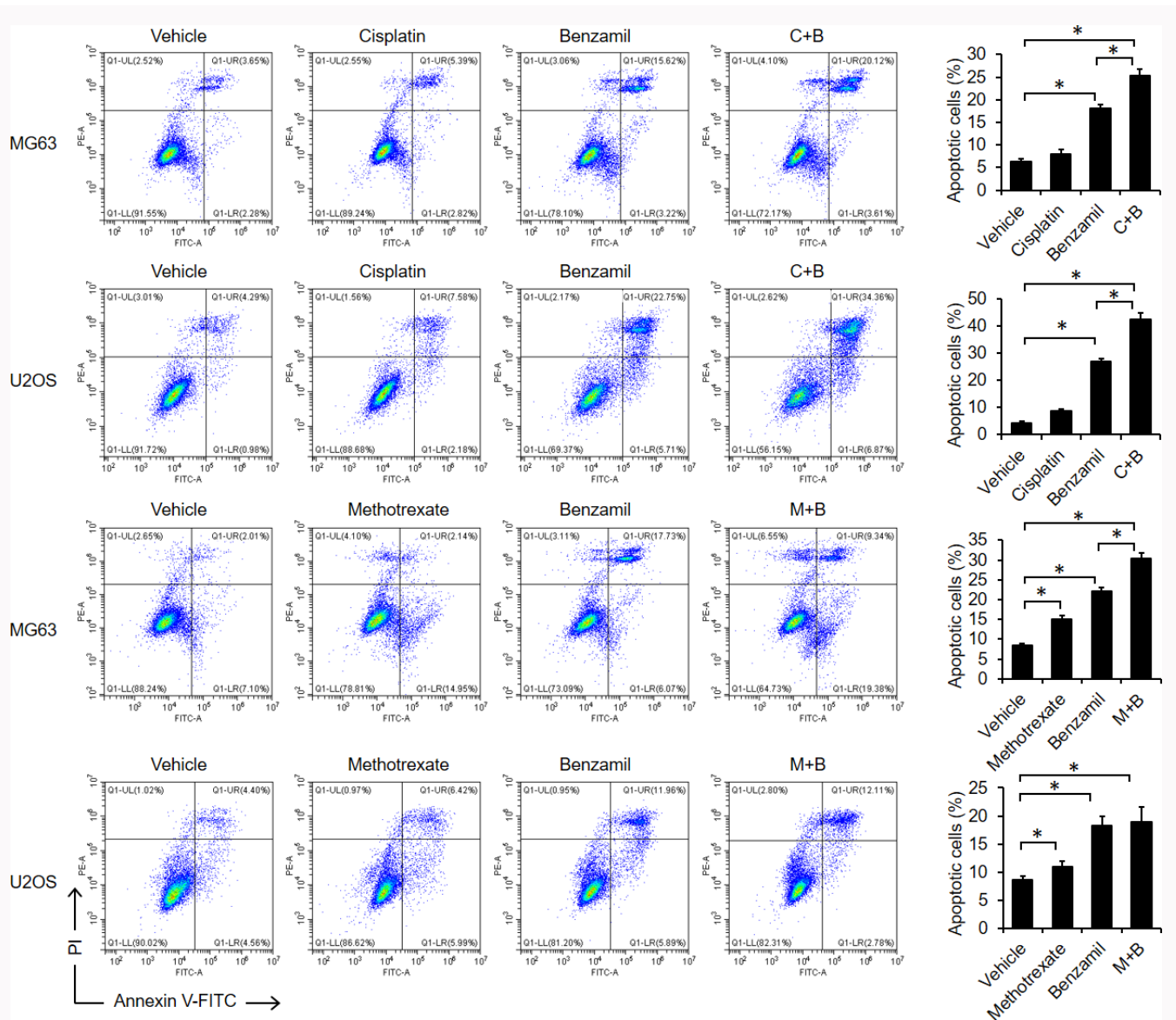


Fig. 7

Benzamil enhances cisplatin-induced apoptosis. MG63 and U2OS cells were pretreated with cisplatin (10 μ M) or methotrexate (30 μ M) for one hour, followed by benzamil (75 μ M) for 24 hours. Apoptosis was analyzed by FITC annexin V/PI double staining. * p < 0.05 comparing indicated groups (one-way analysis of variance). C+B: cisplatin and benzamil; M+B, methotrexate and benzamil. Vehicle: 0.5% dimethyl sulfoxide.

0.1) vs 0.63 (SEM 0.06), p = 0.007, independent-samples t -test) (Figure 6c). However, benzamil only reduced the surface level of integrin α V in U2OS cells (integrin α V: 0 μ M vs 200 μ M: mean 1 (SEM 0.05) vs 0.62 (SEM 0.03), p < 0.001, independent-samples t -test) (Figure 6d). Surprisingly, cell surface expression of integrin β 1 was increased by benzamil treatment in U2OS cells (integrin β 1: 0 μ M vs 200 μ M: mean 1 (SEM 0.05) vs 1.36 (SEM 0.08), p = 0.002, independent-samples t -test).

Benzamil potentiates cisplatin-induced apoptosis

Our in vitro experiments up to this point in the study had consistently demonstrated anti-osteosarcoma activity of benzamil. Therefore, we wanted to further investigate whether benzamil could potentiate cisplatin- and methotrexate-induced apoptosis in osteosarcoma cells. To this end, osteosarcoma cells (MG36 and U2OS) were cotreated with cisplatin/methotrexate and benzamil, and apoptosis was tracked by annexin V/PI double staining assay. The results

showed that both cisplatin and methotrexate treatment alone could only induce apoptosis in a low proportion of the cells (MG63: vehicle vs cisplatin: mean 6.3 (SEM 0.6) vs 8 (SEM 1), p = 0.070, one-way ANOVA; U2OS cells: vehicle vs cisplatin: mean 4.3 (SEM 0.6) vs 8.7 (SEM 0.58), p < 0.001; MG63: vehicle vs methotrexate: mean 8.3 (SEM 0.6) vs 15 (SEM 1), p < 0.001; U2OS cells: vehicle vs methotrexate: mean 8.7 (SEM 0.58) vs 11 (SEM 1), p < 0.05, one-way ANOVA). However, the addition of benzamil could greatly enhance cisplatin-induced apoptosis in both MG63 and U2OS cells (MG63 cells: benzamil vs C+B: mean 18 (SEM 1) vs 25.3 (SEM 1.5), p = 0.002; U2OS cells: benzamil vs C+B: mean 27 (SEM 1) vs 42.3 (SEM 2.5), p < 0.001, one-way ANOVA). However, benzamil only potentiates methotrexate-induced apoptosis in MG63 cells (MG63 cells: benzamil vs M+B: mean 22 (SEM 1) vs 30.3 (SEM 1.5), p < 0.05; U2OS cells: benzamil vs M+B: mean 18.3 (SEM 1.5) vs 19 (SEM 2.6), p = 0.720, one-way ANOVA) (Figure 7).

Discussion

Amiloride is a diuretic used to treat hypokalaemia, hypertension, and heart failure.²⁸ The drug has also been shown to exhibit promising anticancer activity for various types of cancer, including multiple myeloma,²⁸ pancreatic cancer,²⁹ colon cancer,³⁰ and breast cancer.³¹ Its analogue, benzamil, also possesses diuretic activity,¹³ but the anticancer activity of benzamil has not been explored in detail. Only one study has so far demonstrated an anticancer activity of benzamil on human neuroblastoma and astrocytoma cells.¹⁶ In that study, elevation of intracellular calcium was shown to be essential for benzamil-induced cell death.¹⁶ Nevertheless, the anticancer effects and underlying mechanisms of benzamil in other types of cancer cells have not yet been reported. To the best of our knowledge, this is the first study to reveal the anticancer effect of benzamil on human osteosarcoma cells. Furthermore, we determined that the underlying mechanism of this effect most likely involves the inhibition of FAK/STAT3 activation, suppression of mitochondrial function, and alterations to the integrin expression profile.

The MG63 and U2OS cell lines were both derived from osteosarcoma patient samples. However, the two lines differ in terms of their cancer-related phenotypes.³² For instance, MG63 cells exhibit strong clonogenic ability, while the clonogenic ability is relatively weak in U2OS cells.³² Furthermore, the invasive and migratory abilities of U2OS are much stronger than those of MG63 cells.³² Cancer cells with different cancer-related phenotypes usually have different chemosensitivities,³³ but our cytotoxicity (Figure 1) and apoptosis (Figure 2) assays revealed potent anticancer activity of benzamil in both MG63 and U2OS cells. These results suggest that benzamil-induced cytotoxicity is not limited to osteosarcoma cells with certain phenotypes, suggesting that it may have broad potential therapeutic value.

As mentioned above, benzamil induces cytotoxicity in human brain tumour cells by increasing the level of intracellular calcium.¹⁶ This elevation of intracellular calcium is the result of benzamil-mediated suppression of sodium-calcium exchange, which disturbs the balance of intracellular calcium.¹⁶ While the calcium level is also elevated by benzamil in MG63 cells (Figure 3A), this effect is not critical for benzamil-induced cytotoxicity in osteosarcoma cells (Figure 3B).

FAK and STAT3 are often highly expressed in human osteosarcomas,^{25,26} and their high expression is associated with poor prognosis.³⁴ In this work, we found that both FAK and STAT3 were suppressed by benzamil (Figure 4). Furthermore, the respective inhibition of FAK or STAT3 by either Y15 or Stattic could induce apoptosis in osteosarcoma cells (Figure 4d). Thus, it is plausible that benzamil-mediated suppression of FAK and STAT3 might contribute to its cytotoxic activity. Previous studies demonstrated that FAK and STAT3 could facilitate mitochondrial repair, which in turn promotes cell survival in endothelial cells.^{27,35} Thus, we speculated that benzamil-mediated suppression of FAK and STAT3 might impair mitochondrial function in osteosarcoma cells. As predicted, benzamil dramatically reduced mitochondrial membrane potential in both cell lines (Figure 5a). In addition, benzamil reduced the protein levels of anti-apoptotic proteins XIAP, Bcl-2, and Bcl-xL (Figures 5c to 5e). Mitochondrial damage is usually associated with increased ROS production.³⁶ However, we found that ROS levels are

reduced by benzamil (Figure 5f), despite our concurrent evidence that mitochondria damage had occurred (Figure 5a). Since ROS are formed as a byproduct of ATP production by mitochondria,³⁶ we then speculated that the ATP production might be suppressed by benzamil. Intriguingly, our experimental results confirmed our speculation, as intracellular ATP levels were greatly inhibited by benzamil (Figure 5b). Notably, the benzamil-induced detrimental effects on mitochondrial membrane potential and ATP production were stronger in MG63 cells than in U2OS cells (Figures 5a and 5b). As such, we suspect that benzamil may preferentially disrupt mitochondrial function in cells with strong clonogenic ability. Previous work has demonstrated that drug-resistant cancer cells exhibit higher intracellular ATP levels, and ATP depletion can re-sensitize cells to chemotherapeutic agents.^{37,38} In addition, high intracellular ATP levels can trigger cancer metastasis.³⁸ Thus, the ATP-suppressing activity of benzamil could make it a strong candidate for combination therapy with conventional chemotherapeutic agents, as it may help to overcome issues with resistance and metastasis. Anticancer drug combinations can provide several advantages over high doses of single anticancer agents, such as lower chance of drug resistance and fewer side effects.³⁹ Along these lines, we further demonstrated that the anticancer activity of cisplatin and methotrexate may be enhanced by benzamil (Figure 7). Taken together, these observations suggest that the combination of cisplatin/methotrexate and benzamil could provide several advantages over cisplatin or methotrexate alone, such as enhanced anticancer activity and reduced risks of renal and cardiac toxicities from high or accumulated cisplatin and methotrexate dosages.⁴⁰⁻⁴²

Integrins are signalling molecules that act upstream of FAK and STAT3.^{27,43} Moreover, integrins $\alpha 5$,⁴⁴ αV ,⁴⁵⁻⁴⁷ and $\beta 1$ ⁴⁸ are known to be involved in the development of osteosarcoma. We found that benzamil alters the profiles of total protein and/or cell surface integrin expression in both MG63 and U2OS cells (Figure 6). In MG63 cells, benzamil reduces the total protein and cell surface expression levels of integrin $\alpha 5$, αV , and $\beta 1$ (Figures 6a and 6c). However, benzamil does not alter the total protein levels of any measured integrin in U2OS cells (Figure 6b). In addition, cell surface levels of integrin αV were reduced, while integrin $\beta 1$ on the cell surface was elevated by benzamil (Figure 6d). Upregulation of integrin $\beta 1$ is associated with apoptosis resistance and metastasis in osteosarcoma.^{49,50} Moreover, integrin $\beta 1$ can bind to different integrin α subunits to form a variety of heterodimers that may exert a wide variety of diverse biological functions.⁵¹ For instance, the integrin $\alpha 2\beta 1$ heterodimer enhances tumour growth and cancer relapse,⁵² but integrin $\alpha 5\beta 1$ inhibits tumour growth.⁵³ Thus, the precise function of elevated integrin $\beta 1$ in benzamil-induced cytotoxicity in osteosarcoma cells should depend on its association with different integrin α subunits. Further studies will be needed to clarify the potential role of integrin $\beta 1$ and its binding partners in benzamil-induced cytotoxicity toward osteosarcoma cells.

In this study, two osteosarcoma cell lines were used as an in vitro model to validate the anti-osteosarcoma ability of benzamil. Using patient-derived osteosarcoma cells instead of osteosarcoma cell lines might more accurately reflect the response to benzamil in patients. In addition, further in vivo experiments are needed to validate the anti-osteosarcoma

ability of benzamil. Although a previous study demonstrated that 500 µg/kg benzamil does not induce obvious adverse effect in mice,⁵⁴ it is still needed to explore the maximum tolerated dose and possible adverse effect of benzamil in vivo.

References

1. Zhao X, Wu Q, Gong X, Liu J, Ma Y. Osteosarcoma: a review of current and future therapeutic approaches. *Biomed Eng Online*. 2021;20(1):24.
2. Picci P. Osteosarcoma (osteogenic sarcoma). *Orphanet J Rare Dis*. 2007;2:6.
3. Levin AS, Arkader A, Morris CD. Reconstruction following tumor resections in skeletally immature patients. *J Am Acad Orthop Surg*. 2017;25(3):204–213.
4. Saraf AJ, Fenger JM, Roberts RD. Osteosarcoma: accelerating progress makes for a hopeful future. *Front Oncol*. 2018;8:4.
5. Wang H, Ji T, Qu H, et al. Indocyanine green fluorescence imaging may detect tumour residuals during surgery for bone and soft-tissue tumours. *Bone Joint J*. 2023;105-B(5):551–558.
6. Casali PG, Bielack S, Abecassis N, et al. Bone sarcomas: ESMO-PaedCan-EURACAN Clinical Practice Guidelines for diagnosis, treatment and follow-up. *Ann Oncol*. 2018;29(Suppl 4):iv79–iv95.
7. Schwartz CL, Wexler LH, Krailo MD, et al. Intensified chemotherapy with dexrazoxane cardioprotection in newly diagnosed nonmetastatic osteosarcoma: a report from the Children's Oncology Group. *Pediatr Blood Cancer*. 2016;63(1):54–61.
8. Moukengue B, Lallier M, Marchandet L, et al. Origin and therapies of osteosarcoma. *Cancers (Basel)*. 2022;14(14):3503.
9. Prudowsky ZD, Yustein JT. Recent insights into therapy resistance in osteosarcoma. *Cancers (Basel)*. 2020;13(1):83.
10. Wang X, Zhou T, Yang X, et al. DDRGK1 enhances osteosarcoma chemoresistance via inhibiting KEAP1-mediated NRF2 ubiquitination. *Adv Sci (Weinh)*. 2023;10(14):e2204438.
11. Tirtei E, Asaftei SD, Manicone R, et al. Survival after second and subsequent recurrences in osteosarcoma: a retrospective multicenter analysis. *Tumori*. 2018;104(3):202–206.
12. Matsuyama Y, Nakamura T, Yoshida K, et al. Radiodynamic therapy with acridine orange local administration as a new treatment option for primary and secondary bone tumours. *Bone Joint Res*. 2022;11(10):715–722.
13. Sepehrdad R, Chander PN, Singh G, Stier CT. Sodium transport antagonism reduces thrombotic microangiopathy in stroke-prone spontaneously hypertensive rats. *Am J Physiol Renal Physiol*. 2004;286(6):F1185–92.
14. Gupta AK, Arshad S, Poulter NR. Compliance, safety, and effectiveness of fixed-dose combinations of antihypertensive agents: a meta-analysis. *Hypertension*. 2010;55(2):399–407.
15. Hirsh AJ, Sabater JR, Zamurs A, et al. Evaluation of second generation amiloride analogs as therapy for cystic fibrosis lung disease. *J Pharmacol Exp Ther*. 2004;311(3):929–938.
16. Lee YS, Sayeed MM, Wurster RD. Intracellular Ca²⁺ mediates the cytotoxicity induced by bepridil and benzamil in human brain tumor cells. *Cancer Lett*. 1995;88(1):87–91.
17. Franken NAP, Rodermond HM, Stap J, Haveman J, van Bree C. Clonogenic assay of cells in vitro. *Nat Protoc*. 2006;1(5):2315–2319.
18. Matteucci C, Grelli S, De Smaele E, Fontana C, Mastino A. Identification of nuclei from apoptotic, necrotic, and viable lymphoid cells by using multiparameter flow cytometry. *Cytometry*. 1999;35(2):145–153.
19. Su B-C, Mo F-E. CCN1 enables Fas ligand-induced apoptosis in cardiomyoblast H9c2 cells by disrupting caspase inhibitor XIAP. *Cell Signal*. 2014;26(6):1326–1334.
20. Su B-C, Pan C-Y, Chen J-Y. Antimicrobial peptide TP4 induces ROS-mediated necrosis by triggering mitochondrial dysfunction in wild-type and mutant p53 glioblastoma cells. *Cancers (Basel)*. 2019;11(2):171.
21. Kim Y-J, Park S-J, Broxmeyer HE. Phagocytosis, a potential mechanism for myeloid-derived suppressor cell regulation of CD8+ T cell function mediated through programmed cell death-1 and programmed cell death-1 ligand interaction. *J Immunol*. 2011;187(5):2291–2301.
22. Lu ZG, Zhang CM, Zhai ZH. Nucleoplasmin regulates chromatin condensation during apoptosis. *Proc Natl Acad Sci U S A*. 2005;102(8):2778–2783.
23. Lamkanfi M, Kanneganti TD. Caspase-7: a protease involved in apoptosis and inflammation. *Int J Biochem Cell Biol*. 2010;42(1):21–24.
24. Tawa P, Hell K, Giroux A, et al. Catalytic activity of caspase-3 is required for its degradation: stabilization of the active complex by synthetic inhibitors. *Cell Death Differ*. 2004;11(4):439–447.
25. Ren K, Lu X, Yao N, et al. Focal adhesion kinase overexpression and its impact on human osteosarcoma. *Oncotarget*. 2015;6(31):31085–31103.
26. Liu Y, Liao S, Bennett S, et al. STAT3 and its targeting inhibitors in osteosarcoma. *Cell Prolif*. 2021;54(2):e12974.
27. Visavadiya NP, Keasey MP, Razskazovskiy V, et al. Integrin-FAK signaling rapidly and potently promotes mitochondrial function through STAT3. *Cell Commun Signal*. 2016;14(1):32.
28. Rojas EA, Corchete LA, San-Segundo L, et al. Amiloride, an old diuretic drug, is a potential therapeutic agent for multiple myeloma. *Clin Cancer Res*. 2017;23(21):6602–6615.
29. Zheng Y, Yang H, Li T, et al. Amiloride sensitizes human pancreatic cancer cells to erlotinib in vitro through inhibition of the PI3K/AKT signaling pathway. *Acta Pharmacol Sin*. 2015;36(5):614–626.
30. Koo JY, Parekh D, Townsend CM, et al. Amiloride inhibits the growth of human colon cancer cells in vitro. *Surg Oncol*. 1992;1(6):385–389.
31. Leon LJ, Pasupuleti N, Gorin F, Carraway KL. A cell-permeant amiloride derivative induces caspase-independent, AIF-mediated programmed necrotic death of breast cancer cells. *PLoS One*. 2013;8(4):e63038.
32. Lauvrak SU, Munthe E, Kresse SH, et al. Functional characterisation of osteosarcoma cell lines and identification of mRNAs and miRNAs associated with aggressive cancer phenotypes. *Br J Cancer*. 2013;109(8):2228–2236.
33. Sheng S, Margarida Bernardo M, Dzinic SH, Chen K, Heath EI, Sakr WA. Tackling tumor heterogeneity and phenotypic plasticity in cancer precision medicine: our experience and a literature review. *Cancer Metastasis Rev*. 2018;37(4):655–663.
34. Gu H-J, Zhou B. Focal adhesion kinase promotes progression and predicts poor clinical outcomes in patients with osteosarcoma. *Oncol Lett*. 2018;15(5):6225–6232.
35. Banerjee K, Keasey MP, Razskazovskiy V, Visavadiya NP, Jia C, Hagg T. Reduced FAK-STAT3 signaling contributes to ER stress-induced mitochondrial dysfunction and death in endothelial cells. *Cell Signal*. 2017;36:154–162.
36. Cui H, Kong Y, Zhang H. Oxidative stress, mitochondrial dysfunction, and aging. *J Signal Transduct*. 2012;2012:646354.
37. Zhou Y, Tozzi F, Chen J, et al. Intracellular ATP levels are a pivotal determinant of chemoresistance in colon cancer cells. *Cancer Res*. 2012;72(1):304–314.
38. Fiorillo M, Ózsvári B, Sotgia F, Lisanti MP. High ATP production fuels cancer drug resistance and metastasis: implications for mitochondrial ATP depletion therapy. *Front Oncol*. 2021;11:740720.
39. Jaaks P, Coker EA, Vis DJ, et al. Effective drug combinations in breast, colon and pancreatic cancer cells. *Nature*. 2022;603(7899):166–173.
40. Pabla N, Dong Z. Cisplatin nephrotoxicity: mechanisms and renoprotective strategies. *Kidney Int*. 2008;73(9):994–1007.
41. Ali MIM, Imbaby S, Arafat HEK, Maher SA, Kolieb E, Ali SM. Cardioprotective and renoprotective effects of venlafaxine on cisplatin-induced cardiotoxicity and nephrotoxicity in rats. *Life Sci*. 2023;320:121561.
42. Cheng Y, Chen Y, Zhao M, Wang M, Liu M, Zhao L. Metabolomic profiling reveals the mechanisms underlying the nephrotoxicity of methotrexate in children with acute lymphoblastic leukemia. *Pediatr Blood Cancer*. 2023;70(10):e30578.
43. Ren Y, Liu W, Zhang L, et al. Milk fat globule EGF factor 8 restores mitochondrial function via integrin-mediated activation of the FAK-STAT3 signaling pathway in acute pancreatitis. *Clin Transl Med*. 2021;11(2):e295.
44. Liu X-Z, Li C-J, Wu S-J, Shi X, Zhao J-N. Involvement of α5 integrin in survivin-mediated osteosarcoma metastasis. *Asian Pac J Trop Med*. 2016;9(5):478–483.
45. Huang Y, Lin Z, Zhuang J, Chen Y, Lin J. Prognostic significance of alpha V integrin and VEGF in osteosarcoma after chemotherapy. *Onkologie*. 2008;31(10):535–540.
46. Tome Y, Yano S, Sugimoto N, et al. Use of αv integrin linked to green fluorescent protein in osteosarcoma cells and confocal microscopy to image molecular dynamics during lung metastasis in nude mice. *Anticancer Res*. 2016;36(8):3811–3816.

47. Li ZQ, Deng LR, Li YG, Wang YJ. MiR-139 inhibits proliferation, migration and invasion of osteosarcoma cell line MG63 via down-regulating integrin subunit alpha V(ITGAV). *Tissue Cell*. 2022;75:101720.
48. Kimura H, Tome Y, Momiyama M, et al. Imaging the inhibition by anti- β 1 integrin antibody of lung seeding of single osteosarcoma cells in live mice. *Int J Cancer*. 2012;131(9):2027–2033.
49. Li R, Shi Y, Zhao S, Shi T, Zhang G. NF- κ B signaling and integrin- β 1 inhibition attenuates osteosarcoma metastasis via increased cell apoptosis. *Int J Biol Macromol*. 2019;123:1035–1043.
50. Mao LW, Wang L, Xu JK, Zou J. The role of integrin family in bone metabolism and tumor bone metastasis. *Cell Death Discov*. 2023;9(1):119.
51. Desgrosellier JS, Cheresh DA. Integrins in cancer: biological implications and therapeutic opportunities. *Nat Rev Cancer*. 2010;10(1):9–22.
52. Wei D, Li C, Ye J, Xiang F, Liu J. Extracellular collagen mediates osteosarcoma progression through an integrin α 2 β 1/JAK/STAT3 signaling pathway. *Cancer Manag Res*. 2020;12:12067–12075.
53. Varner JA, Emerson DA, Juliano RL. Integrin alpha 5 beta 1 expression negatively regulates cell growth: reversal by attachment to fibronectin. *Mol Biol Cell*. 1995;6(6):725–740.
54. Ydegaard R, Andersen H, Oxlund CS, et al. The acute blood pressure-lowering effect of amiloride is independent of endothelial ENaC and eNOS in humans and mice. *Acta Physiol (Oxf)*. 2019;225(1):e13189.

Author information

M-C. Lin, BS, Graduate Student

G-Y. Chen, College Student

School of Medical Laboratory Science and Biotechnology, College of Medical Science and Technology, Taipei Medical University, Taipei, Taiwan.

H-H. Yu, MD, PhD, Surgeon and Assistant Professor, Division of General Surgery, Department of Surgery, Wan Fang Hospital, Taipei Medical University, Taipei, Taiwan; Division of General Surgery, Department of Surgery, School of Medicine, College of Medicine, Taipei Medical University, Taipei, Taiwan.

P-L. Hsu, PhD, Assistant Professor, Department of Anatomy, School of Medicine, College of Medicine, Kaohsiung Medical University, Kaohsiung, Taiwan; Department of Medical Research, Kaohsiung Medical University Hospital, Kaohsiung, Taiwan.

C-W. Lee, PhD, Assistant Professor, Department of Nursing, National Tainan Junior College of Nursing, Tainan, Taiwan.

C-C. Cheng, MS, Research Assistant, Division of General Surgery, Department of Surgery, Wan Fang Hospital, Taipei Medical University, Taipei, Taiwan.

S-Y. Wu, PhD, Postdoctoral Researcher, Department of Cancer Biology, Wake Forest Baptist Medical Center, Wake Forest University, Winston-Salem, North Carolina, USA.

B-S. Pan, PhD, Senior Research Associate, Department of Pathology, Duke University School of Medicine, Durham, North Carolina, USA.

B-C. Su, PhD, Associate Professor, Department of Anatomy and Cell Biology, School of Medicine, College of Medicine, Taipei Medical University, Taipei, Taiwan; Graduate Institute of Medical Sciences, College of Medicine, Taipei Medical University, Taipei, Taiwan.

Author contributions

M-C. Lin: Data curation, Investigation, Validation, Writing – original draft.

G-Y. Chen: Data curation, Formal analysis, Investigation.

H-H. Yu: Conceptualization, Data curation, Funding acquisition, Writing – original draft.

P-L. Hsu: Investigation.

C-W. Lee: Investigation.

C-C. Cheng: Data curation, Investigation.

S-Y. Wu: Writing – review & editing.

B-S. Pan: Writing – review & editing.

B-C. Su: Funding acquisition, Investigation, Writing – original draft, Writing – review & editing.

Funding statement

The authors disclose receipt of the following financial or material support for the research, authorship, and/or publication of this article: funding from the Ministry of Science and Technology (MOST, Taiwan; MOST 109-2320-B-038-010-MY2, 110-2320-B-038-023-), received by B-C. Su. This research was also funded by Taipei Municipal Wan Fang Hospital (110TMU-WFH-20), received by H-H. Yu. No benefits in any form have been received or will be received from a commercial party related directly or indirectly to the subject of this article.

ICMJE COI statement

B-C. Su reports funding from the Ministry of Science and Technology (MOST, Taiwan; MOST 109-2320-B-038-010-MY2, 110-2320-B-038-023-), related to this study. H-H. Yu reports funding from Taipei Municipal Wan Fang Hospital (110TMU-WFH-20), related to this study.

Data sharing

All data generated or analyzed during this study are included in the published article and/or in the supplementary material.

Acknowledgements

The authors thank Marcus Calkins for the English language editing.

Open access funding

The authors report that they received open access funding for their manuscript from the Ministry of Science and Technology (MOST, Taiwan; MOST 109-2320-B-038-010-MY2, 110-2320-B-038-023-).

© 2024 Lin et al. This is an open-access article distributed under the terms of the Creative Commons Attribution Non-Commercial No Derivatives (CC BY-NC-ND 4.0) licence, which permits the copying and redistribution of the work only, and provided the original author and source are credited. See <https://creativecommons.org/licenses/by-nc-nd/4.0/>